Journal of Structural Geology, Vol. 13, No. 1, pp. 49 to 62, 1991
Printed in Great Britain

0191-8141/91 $03.00+0.00

Paleostresses associated with faults of large offset

STEVEN WOJTAL

Department of Geology, Oberlin College, Oberlin, OH 44074, U.S.A.

and

JONATHAN PERSHING

Department of Geology and Geophysics, Pillsbury Hall, University of Minnesota, Minneapolis, MN 55455, U.S.A.

(*Received* 13 *July* 1989; *accepted in revised form* 11 *April* 1990)

Abstract—In order to test empirically the limitations of paleostress analysis, we used Etchecopar's computer program to compute the orientations and relative magnitudes of paleostress principal values in two southern Appalachian (U.S.A) thrust zones from minor fault and slickenside attitudes. In both thrust zones, faults are closely spaced, many faults have offsets whose magnitudes exceed the distance to adjacent faults of comparable size, and deformation was strongly non-coaxial. While even in the less-deformed thrust zone bulk strains due to fault movement have axial ratios as high as 10:1, nearly 75% of the fault–slickenside pairs in each thrust zone conform with paleostress tensors that indicate: (1) sequential transport-parallel compression, transport-parallel extension and extension oblique to transport; and (2) low resolved shear stresses on the thrusts. Finite strains measured in one thrust zone share a principal plane with the first two tensors, and the inclinations of the paleostress and finite strain principal directions in that plane are consistent with thrust-parallel shearing. Relative magnitudes of paleostress and strain principal values do not correlate well. Moreover, the locations and inferred origins of fault–slickenside pairs inconsistent with paleostress tensors suggest that stresses in rocks between faults were not, as is assumed in paleostress analyses, uniform; this complexity may also occur in faulted rocks where bulk strains are small. Paleostress tensors from rocks with large bulk strains may be viable, but they must be interpreted cautiously.

INTRODUCTION

TRADITIONAL analyses of fault systems use a two-dimensional Coulomb criterion for failure to guide inferences about the stresses responsible for faults (cf. Anderson 1951). Faults in natural arrays rarely occur, however, in the simple conjugate sets predicted by Anderson's theory (Arthaud 1969, Reches 1978, Aydin & Reches 1982). Faults in three-dimensional deformations may conform with the Coulomb criterion (Reches & Dieterich 1983), but, because rocks are inherently anisotropic, faults often develop at angles to principal stress directions other than those predicted by analyzing isotropic media (Handin 1969, Gretener 1972). Slip on natural faults may not be frictional if the slip rate is sufficiently low that other deformation mechanisms, particularly diffusive mechanisms, prevail along the fault surfaces (Elliott 1976, Rutter & Mainprice 1978, Shimamoto 1986).

Wallace (1951) and Bott (1959) suggested that faults follow pre-existing surfaces with low cohesion, with fault slip parallel to the maximum resolved shear stress. Arthaud (1969) argued that slip directions on numerous faults, as indicated by slickensides, define directions of bulk shortening and elongation for discontinuous deformations. Carey & Brunier (1974) reversed Bott's analysis and computed orientations for the principal directions and relative magnitudes for the principal values of paleostress tensors from the strikes and dips of faults, the pitches of slickensides on those faults and the relative senses of movement on the faults. Angelier & Mechler (1977), Armijo & Cisternas (1978), Angelier (1979, 1984), Carey (1979), Etchecopar *et al.* (1981), Angelier *et al.* (1982), Ellsworth (1982), Michael (1984), and Reches (1987) refined and computerized this basic approach; their analyses of field data, synthetic structural data, and earthquake focal mechanisms suggest that this approach estimates reliably tectonic stresses. (We refer to the numerical vector and tensor outputs of inverse stress programs as 'paleostress vectors', 'paleostress tensors' or 'paleostresses' to distinguish them from traction vectors and stress tensors derived analytically.)

Standard paleostress analyses examine fault-accommodated deformation that conforms with the following conditions: stresses were homogeneous during deformation, deformation was coaxial, fault slip was small relative to fault spacing, and no plastic deformation accompanied fault slip. These conditions are to some degree violated in all natural fault arrays used for paleostress analysis. For example, spatial variations in stresses appear in subsets of fault populations (cf. Angelier 1984). Stylolites and tension gashes show that mechanisms other than fault slip accommodate deformation in faulted rocks (Arthaud & Mattauer 1969, Etchecopar *et al.* 1981, Angelier 1984). Michael (1984) even used a fault-slip paleostress technique to analyze bedding slip in folds. There is, then, latitude in how strictly these initial conditions apply even in cases where paleostress analyses have been successful.

One purpose of this contribution is to examine the

extent to which paleostress analyses must adhere to these initial conditions to remain valid. If, indeed, the criteria discussed above need not be rigidly adhered to, we will have access to a powerful tool to examine deformation in regions where, at present, there is little chance of assessing the local and regional stress histories. The examination presented in this paper is entirely empirical; we make no theoretical evaluation of the validity of inverse stress assumptions.

We use an unpublished computer program (Etchecopar *et al.* 1981 outlined the algorithm for the program) to compute paleostress tensors for two thrust zones. Paleostress tensors are apparently well-defined in both thrust zones. Where fault-accommodated deformation is mesoscopically homogeneous (Wojtal & Mitra 1986), paleostress and measured finite strain tensors share a principal plane. Paleostress principal values conform generally with the senses of offset on faults and other kinematic indicators. The orientations and magnitudes of paleostress principal vectors do not, however, correlate precisely with strain principal values. Our results indicate that, in rocks that depart widely from the initial conditions listed above and perhaps some other cases, 'paleostress analysis' is most effective at identifying subsets of faults that together accommodated individual deformation increments. Calculated 'paleostress principal directions' are, then, directions of incremental shortening and elongation.

In the thrust zones we examine, the incremental shortening and elongation directions (1) were markedly different at different times during the thrust-zone evolution, and (2) suggest that the major thrust surfaces had low resolved shear stresses. Our second inference is consistent with recent reports of principal stresses nearly normal to, and low shear stress magnitudes resolved on, major strike-slip fault zones (cf. Mount & Suppe 1987). Such stress attitudes may, apparently, exist in close proximity to major faults.

GEOLOGIC SETTING OF MESOSCOPIC FAULT ARRAYS

Our fault surface and slickenside data come from arrays of mesoscopic faults near two southern Appalachian (U.S.A) foreland fold-and-thrust belt thrusts. Faults in each array are elements in a pervasive mesoscopic fabric in sedimentary strata adjacent to these thrusts (Wojtal 1982, 1986). Minor faults do not cut the thrusts, and they exhibit mutually cross-cutting patterns consistent with formation during thrust movement (Woodward *et al.* 1988).

Cumberland Plateau (CP) thrust zone

Our first data set comes from the mesoscopic fault array in strata in the hangingwall of the Cumberland Plateau (CP) thrust near Dunlap, Tennessee (Fig. 1a) (Harris & Milici 1977). The CP thrust has a simple, stepped shape (Milici 1963) (Fig. 1b). To the west, Pennsylvanian strata in a hangingwall flat lie on slightly younger Pennsylvanian strata in a footwall flat (Stearns 1954). Where the CP thrust steps down from this upper glide horizon to the regional detachment in Cambrian strata, Ordovician carbonates in a hangingwall ramp lie on Mississippian units near the crest of the footwall ramp. Displacement is 2–3 km at the ramp, but decreases up the dip of the thrust to 300–1000 m along the upper glide horizon (Harris & Milici 1977).

Where the upper glide horizon crops out near Dunlap, the CP thrust has a dip direction/dip of 110/02°. Within 100 m of the thrust, mesoscopic faults that formed during sheet transport toward the west-northwest cut the mainly flat-lying hangingwall strata at low (<45°) or high (>45°) angles to bedding (Harris & Milici 1977, Wojtal 1986) (Fig. 2). Most low-angle faults strike roughly parallel to the strike of the thrust, dip toward the east (a few dip to the west) and have reverse offsets of bedding. Slickensides on low-angle faults have pitches close to 90°. The density of, and mean offsets on, low-angle faults decrease with distance from the thrust (Wojtal & Mitra 1986), and, as we outline below, the kinematics of high-angle faults change with position relative to the thrust. High-angle faults cut across low-angle faults where both occur together.

We divided the intensively-faulted strata adjacent to the CP thrust into three regions where the types of faults that constitute the array, their attitudes and cross-cutting patterns are approximately uniform (Fig. 2). Strata within 10 m of the CP thrust compose the first region, CPLOW. In that region, large regularly-spaced high-angle faults cut and offset closely-spaced low-angle faults. High-angle faults in the CPLOW region typically dip to the west, often with steeper dips nearer the thrust than elsewhere along their lengths. Slickensides on high-angle faults here typically have pitches close to 0°, and slip on these faults produced mainly normal but some reverse offsets of bedding and low-angle faults. Strata between 10 and 50 m from the thrust compose a second region, CPMID. In CPMID, low-angle faults predominate; clusters of high-angle faults appear sporadically in transects parallel to thrust transport. High-angle faults in this middle region dip either west or east, have down-slip slickensides, and normal offsets of bedding and low-angle faults. At the stratigraphic and structural top of the middle region is a laterally persistent coal seam. West-dipping high-angle faults with down-dip slickensides and normal offsets predominate in strata above the coal seam, which compose a third region, CPUPP.

In the strata adjacent to the CP thrust at Dunlap, the attitudes of faults, slickenlines, fold hinges and fold hinge lines indicate that a plane perpendicular to the thrust and parallel to transport is a plane of mirror symmetry, inferred to be a principle plane for deformation (Wojtal 1986). Spatial gradients of displacements of fault-bounded blocks are roughly constant, and values of bulk strains due to movement on minor faults are well defined (Wojtal 1986, 1989a). For strata within 10 m of the CP thrust, the bulk strain principal shortening direction is 280/60° (bearing/plunge) and the bulk

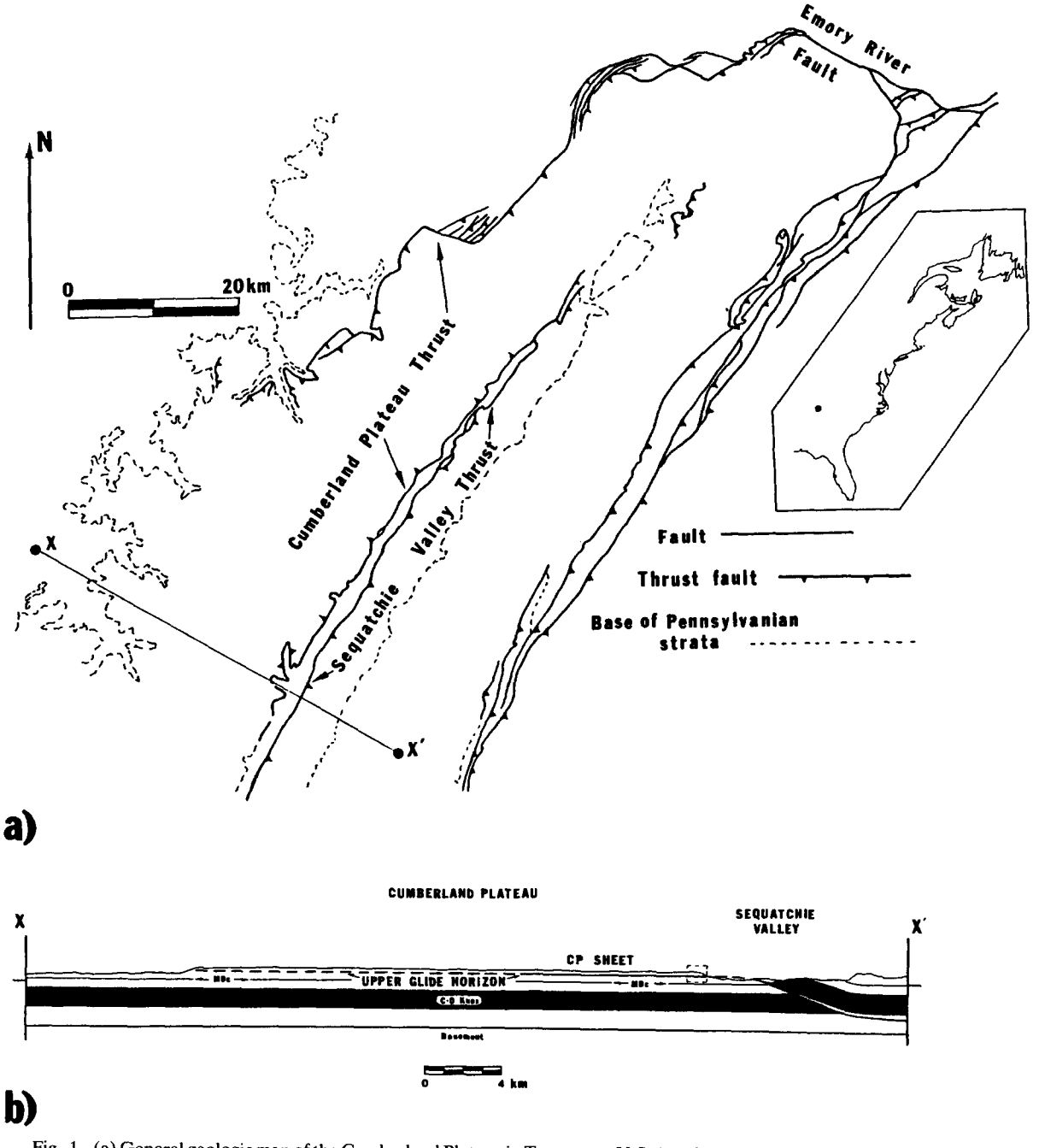

Fig. 1. (a) General geologic map of the Cumberland Plateau in Tennessee, U.S.A., after Milici (1963). Filled circle on inset shows location of the exposure. X–X′ = line of section in (b). (b) Cross-section of the CP thrust (from Wojtal 1982); location of the Dunlap exposures outlined by dashed lines.

strain principal elongation is 110/30°. Axial ratios in the principle plane (measured with the techniques outlined in Wojtal 1989a) are 5:1 to 10:1 in the CPLOW region, and the ratio of area in the section plane after deformation to area in the section plane before deformation is about 0.9. In the CPMID region (between 10 and 50 m from the CP thrust), the bulk strain principal shortening direction is about 280/40° and principal elongation direction is 110/50°. Axial ratios in the section plane are 1.3:1 to 1.5:1, and the ratios of area in the section plane after deformation to area in the section plane before deformation are close to 1.0. In the CPUPP region (above the coal seam), the bulk strain principal elongation direction is 280/25°, the bulk strain principal shortening direction is 110/65°, the axial ratio is about 1.3:1 and the area ratio is about 1.0.

Hunter Valley (HV) thrust zone

Our second data set comes from pervasively faulted Cambrian carbonates in the hangingwall of the Hunter Valley (HV) thrust near Duffield, Virginia (Fig. 3a). Strata in the hangingwall of the HV thrust originated in the regional décollement zone for this portion of the Valley and Ridge Province (Rich 1934, Rodgers 1970, pp. 47–48); their position here on Devonian shales at the crest of a major footwall ramp indicates a net displacement of about 16 km toward the northwest (Fig. 3b). A

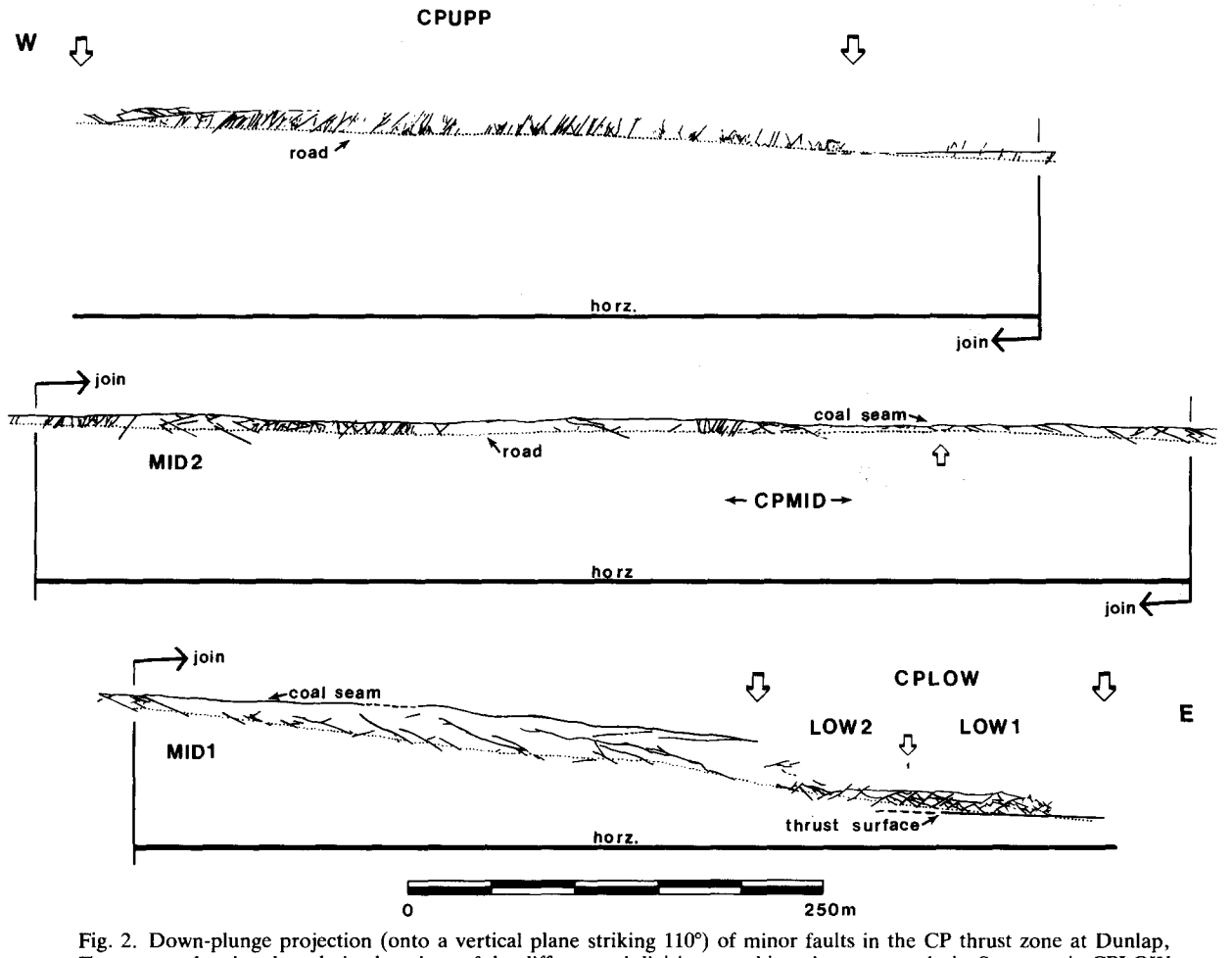

Fig. 2. Down-plunge projection (onto a vertical plane striking 110°) of minor faults in the CP thrust zone at Dunlap, Tennessee, showing the relative locations of the different subdivisions used in paleostress analysis. Structure in CPLOW and CPMID subdivisions from Wojtal (1982); structure in CPUPP modified from Harris & Milici (1977).

banded cataclasite at least 20 cm thick occurs along the HV thrust at this location.

The HV thrust at Dunlap dips about 25° toward 140°; strata above the thrust have, on average, the same dip and dip direction as the thrust. Minor faults again cut the hangingwall strata at low angles (<45°) or high angles (>45°) to bedding, with high-angle faults again later than low-angle faults (Fig. 4). Low-angle faults strike parallel to the thrust, dip toward the southeast (a few dip NW), and have reverse offsets of bedding. Slickensides on them have pitches close to 90°. The density of, and mean offsets on, low-angle faults again decrease with distance from the thrust, and high-angle faults again change their attitudes and kinematics with changes in position relative to the thrust.

Immediately above the HV thrust are pervasively faulted strata of the Cambrian Rutledge Limestone. The types of mesoscopic faults that constitute the array, their attitudes and their cross-cutting patterns are similar in all Rutledge strata exposed near Duffield. The latest faults in this array are regularly-spaced high-angle faults with strikes of 110° or 350° (±60° to the thrust strike). Slickensides on these faults have pitches ranging from 0° to 45°, and slip on the faults produced both normal and reverse offsets. These oblique-slip faults cut and offset high-angle faults that strike parallel to the thrust, have slickensides whose pitches are either 0° or 90°, and usually have normal offsets. Both types of high-angle faults cut and offset low-angle faults. Restoring separate segments of low-angle faults by reversing high-angle fault offsets indicates that many low-angle faults have stepped shapes. Strata between faults are folded due to movement on step-shaped faults, folded due to 'drag' on faults, and cut by numerous mineral-filled fractures and microfaults.

We divided the deformed Rutledge Limestone into three regions to facilitate paleostress analysis (Fig. 4). The lowest region (HVRUT1) comprises strata between the HV thrust and a laterally-persistent, large-displacement contraction fault about 15 m above the thrust. The second region (HVRUT21 and HVRUT22) comprises strata between the contraction fault 15 m above the thrust and a second laterally-persistent, large-displacement contraction fault about 40 m above the thrust. The third region (HVRUT3) comprises the exposed Rutledge strata above the second large contraction fault (40–70 m from the thrust). Fault spacing is lowest and the density of mineral-filled fractures and microfaults is greatest in the region immediately above the thrust; fault spacing is greater and the fracture/microfault density lower in regions farther from the thrust (Wojtal & Mitra 1986).

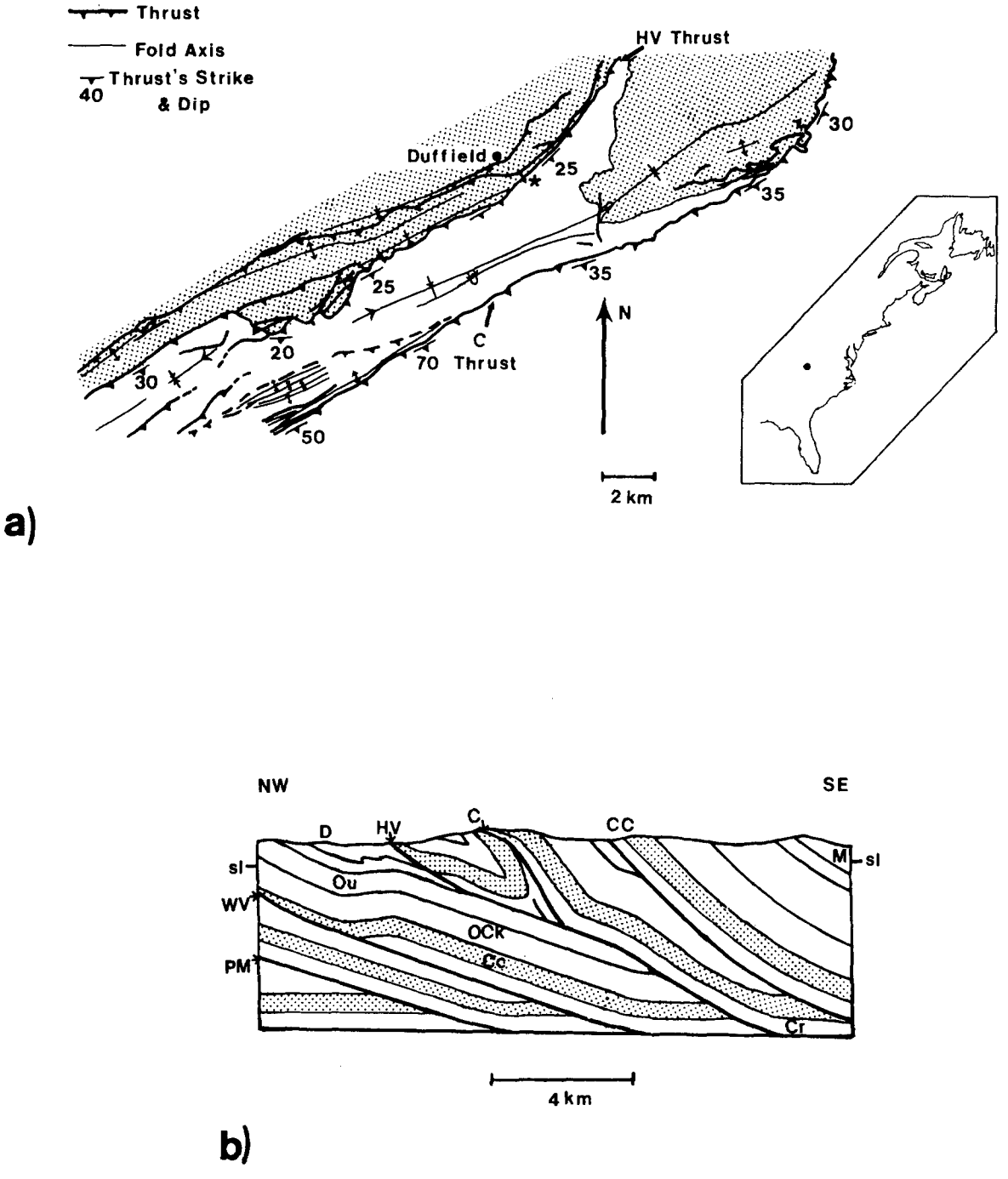

Fig. 3. (a) Map showing the general geology of the vicinity of Duffield, Virginia, and traces and attitudes of the Hunter Valley (HV) and Clinchport (C) thrusts (from Wojtal 1989b). Filled circle on inset gives location of the exposure. ★ is the location of the HV thrust exposure cited in the text; stipple denotes Ordovician and younger strata. (b) Cross-section based on down-plunge projections of structures in the vicinity of Duffield, Virginia (from Wojtal 1989b). PM = Pine Mountain thrust; WV = Wallen Valley thrust; CC = Copper Creek thrust; Cr, Cc, OCK, Ou, D and M denote Cambrian Rome Formation, Cambrian Conasauga Group, Cambro-Ordovician Knox Group, Middle and Upper Ordovician, Devonian and Mississippian strata, respectively.

About 15–30 m of fissile, siliciclastic shale, the Rogersville Shale, separate a second limestone unit, the Maryville Limestone, from the Rutledge Limestone (Fig. 4). The shale is mostly covered, but has isolated tight folds where exposed. Low- and high-angle faults cut Maryville strata up to 300 m above the HV thrust. Low-angle faults in the Maryville Limestone (HVMAR1) resemble those found closer to the thrust, although antithetic (NW) dips are more common and fault spacing greater in Maryville strata. High-angle faults in the Maryville strike parallel to the HV thrust, have slickensides whose pitches are close to either 0° or 90°, and usually have normal offsets.

On the basis of the types of faults that constitute the array, their attitudes relative to the HV thrust and their cross-cutting patterns, the fault array near the HV thrust resembles that in strata near the CP thrust. Slip was preferentially partitioned on a small number of minor faults in strata near the HV thrust, however, and displacement gradients measured over distances of several

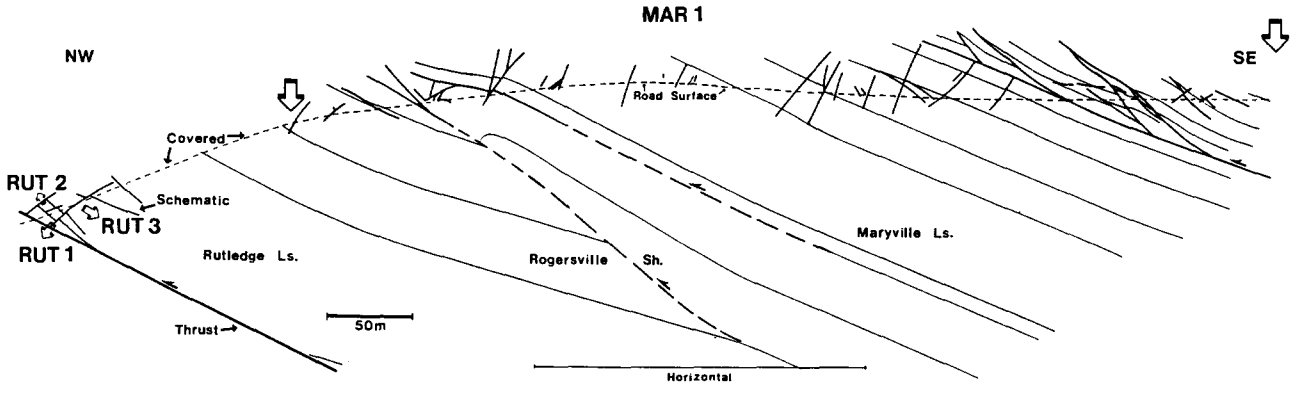

Fig. 4. Down-plunge projection (onto a plane whose dip direction and dip are 045/85°) of minor faults in the HV thrust zone at Duffield, Virginia, showing the relative locations of the different subdivisions used in paleostress analysis.

tens of meters are not constant (Wojtal & Mitra 1986). We were unable, therefore, to calculate bulk strain values in these rocks. The magnitudes of slip on individual faults, the high density of mineral-filled fractures and microfaults and the occurrence of a banded cataclasite along the thrust indicate that strain values near the HV thrust exceed those in the faulted strata near the CP thrust (Wojtal & Mitra 1986).

TECHNIQUES FOR PALEOSTRESS ANALYSIS

The available programs for determining paleostress tensors from fault populations have in common numerical computation of a reduced stress tensor involving four unknowns: the three principal stress directions and a stress ratio $R = (\sigma_2 - \sigma_3)/(\sigma_1 - \sigma_3)$. They require that the following conditions be met (cf. Etchecopar *et al.* 1981, Angelier 1984, Michael 1984, Reches 1987): (1) the stress tensor was symmetric and stresses were homogeneous throughout the region of interest; (2) fault slip paralleled the maximum resolved shear stress acting upon the faults surfaces; (3) faults preserve the geometry that they had during the period of faulting; and (4) faults and slickensides in a population have a variety of attitudes and therefore clearly constrain paleostresses.

Our analysis encountered difficulties in conforming exactly with these conditions that are common to all paleostress studies. For example, strata in these thrust zones may have deformed inhomogeneously, either from multiple deformation episodes (i.e. stress axes rotated) or when faults rotated relative to stress orientations. Cross-cutting relationships suggest that strata in these thrust zones deformed in response to more than one stress system. Moreover, some faults have curved or overprinting multiple slip fibers. The technique outlined by Etchecopar *et al.* (1981) discerns subsets of faults compatible with successive paleostress tensors in multiply deformed rocks, and has been used with success elsewhere (cf. Kleinspehn *et al.* 1989). Our ability to isolate individual homogeneous tensors from data helps to retain compatibility with the conditions outlined above. We used the different slickensides on faults with multiple slip fibers as distinct fault–slickenside pairs in our analysis. Since slip fibers formed during later slip increments may erase early-formed lineations (Ramsay & Huber 1983, p. 258), slickensides on faults with single lineations probably only record the movement direction for the last deformation increment in which that fault was active.

There are other difficulties in interpreting the movement directions on faults and relating them to resolved shear stresses. Slickensides on faults in our samples are calcite or quartz mineral fibers, or less commonly Means's (1987) ridges-and-grooves or features resembling Petit's (1987) PO-type markings. Despite the available criteria for inferring movement sense from non-fibrous slickensides (Tjia 1967, Petit 1987, Gamond 1987, Means 1987), visually similar markings may form by different slip modes in opposite directions (Tjia 1964, Norris & Barron 1968, Gay 1970). To counter difficulties in determining reliably the sense of movement from non-fibrous fault markings, we used fault–non-fibrous slickenside pairs only where offset markers indicate the movement sense. We discuss below the effects this choice has on interpreting our measured paleostresses.

Paleostress analysis assumes that slickenlines depict unequivocally the directions of the resolved shear stress on a given plane. If displacements are small and stresses are homogeneous, there is little temporal deviation in the orientation of the resolved shear stress on an individual fault surface. Observed slickenlines are then likely to parallel this resolved shear stress vector. The dilemma in our analysis is that individual slickenlines may not parallel the resolved shear stresses on a plane at all times during deformation. For example, if a fault rotates relative to fixed stresses, or if the stresses rotate relative to a fixed fault, the maximum resolved shear stress on that plane will change with time. An increment of slip is needed to generate a slickenline on a fault plane; this incremental displacement correlates with a strain increment. The principal shortening and elongation directions of this strain increment are, of course, parallel to compression and elongation directions in materials that obey Levy–Mises equations (Ford 1963, p. 410, Arthaud 1969). Because we use only fault–

slickenline pairs where measurable offsets corroborate the sense of movement of slip fibers, and because rocks in these thrust zones may have significant plastic strains not due to fault slip, our paleostress principle directions are best interpreted as directions of shortening and elongation for individual deformation increments.

Our data do comply with the requirement that a variety of fault orientations be measured, although particular fault attitudes do recur in our samples and may reduce the accuracy of measured paleostress tensors. In the arrays we consider here, conformity with the preconditions for paleostress analysis is reduced further by the thrust-zone setting and the large offsets on many faults as follows.

(1) Multiple slip fibers on individual faults, systematic cross-cutting patterns in the arrays, and the formation, rotation and renewed formation of veins in the HV cataclasite show that successive strain increments in the thrust zones were not coaxial (Wojtal & Mitra 1986).

(2) Where the spacing between faults is small relative to measured offsets on faults, movement on one fault may change the attitude of neighboring faults. Even if the far-field stresses did not change with fault slip, stresses on individual faults would change as slip accrued on neighboring faults.

(3) When net slip on non-planar faults is large, fault-bounded blocks rotate relative to a fixed reference frame, and smaller faults within fault-bounded blocks rotate relative to fixed stress principal directions.

(4) Where strata within fault-bounded blocks are folded and cut by microfaults and fractures, fault-bounded blocks change shape during deformation. The large faults bounding these blocks change orientations relative to fixed stresses as blocks changed shape.

(5) For faults with curved slip fibers, either stress principal directions and principal values changed, or minor faults rotated relative to stresses during fault slip (Mandal & Chakraborty 1989).

Despite this lack of conformity with the conditions normally required for paleostress analysis, fault arrays in the different regions of the CP and HV thrust zones yield well-defined paleostress tensors (see Figs. 5 and 6). Output from the version of the program we use (Etchecopar personal communication 1986) includes the orientations and relative values of the best-fit principal values, errors in these parameters, a histogram of the number of fault–slickenside pairs vs angular deviation, and Mohr circles showing how different fault–slickenside pairs contribute to defining the paleostress tensor. The histograms and Mohr circles calculated in each iteration are particularly helpful in assessing the robustness of paleostress tensors.

As detailed by Etchecopar *et al.* (1981), we used the histograms from different iterations to distinguish data compatible with a paleostress tensor from 'residual' data pairs. In a well-constrained paleostress tensor, large numbers of data pairs have angular deviations less than 17°, and frequencies of occurrence fall rapidly as angular deviation rises. Most of our measured tensors have histograms like this, and our results are robust in that we get similar measured tensors when we specify that different percentages (i.e. 30%, 40% or 50% of the data) be used to define each tensor. When we specify that the program use a larger fraction than an arbitrary threshold value (typically about 50%) to compute a paleostress tensor, internal errors increase. We recognize the errors because: (1) principal values and orientations change as the threshold value we chose increases; (2) there are nearly as many data pairs with large angular deviations as those with small angular deviations; (3) the program uses many fault–slickenside pairs compatible with subsequent tensors to define this first tensor. Thus the program separates effectively distinct subsets of data pairs that can, from a geometric standpoint alone, accommodate distinct homegeneous bulk shortening and elongation increments.

Paleostress tensors calculated for strata adjacent to the CP thrust, which has small net displacement, indicate either (1) thrust-parallel and transport-parallel shortening with subvertical elongation, or (2) thrust-parallel and transport-parallel elongation with subvertical shortening. Cross-cutting patterns in this fault array indicate that the transport-parallel shortening preceded transport-parallel elongation. Nearly half of the total number of pairs define one tensor in the CP data, and about half of the remaining data pairs define another tensor in these data (Fig. 5). As in many other paleostress analyses (cf. Kleinspehn *et al.* 1989), nearly one quarter of the fault–slickenside pairs are inconsistent with measured paleostress tensors unless one allows angular deviations to exceed 30°. Paleostress tensors calculated for the fault array in strata adjacent to the HV thrust, which has a large net displacement, also indicate transport-parallel shortening and transport-parallel extension. Nearly 75% of the total number of data pairs again conform with measured paleostress tensors, but the calculated errors in the orientation of principal paleostresses in the HV thrust zone are larger. It is noteworthy that percentages of the data that conform with measured paleostress tensors do not change appreciably as bulk strains increase, but that the calculated errors increase as greater fractions of the fault populations have 'large' slip.

DISCUSSION

Given the large displacements on some faults in these arrays and non-coaxial nature of deformation in these thrust zones, it is not surprising that 25% of our data do not conform with any paleostress tensor. It is curious, however, that the fault–slickenside measurements that define paleostress tensors typically are those from large-offset faults (Fig. 7). These faults divide strata into separate 'blocks' whose relative motion accommodates most deformation (Wojtal & Mitra 1986). Slickensides on large-offset faults apparently record slip increments compatible with contemporaneous (and relatively late) deformation increments. Faults presumably remained active as long as they were favorably oriented for slip,

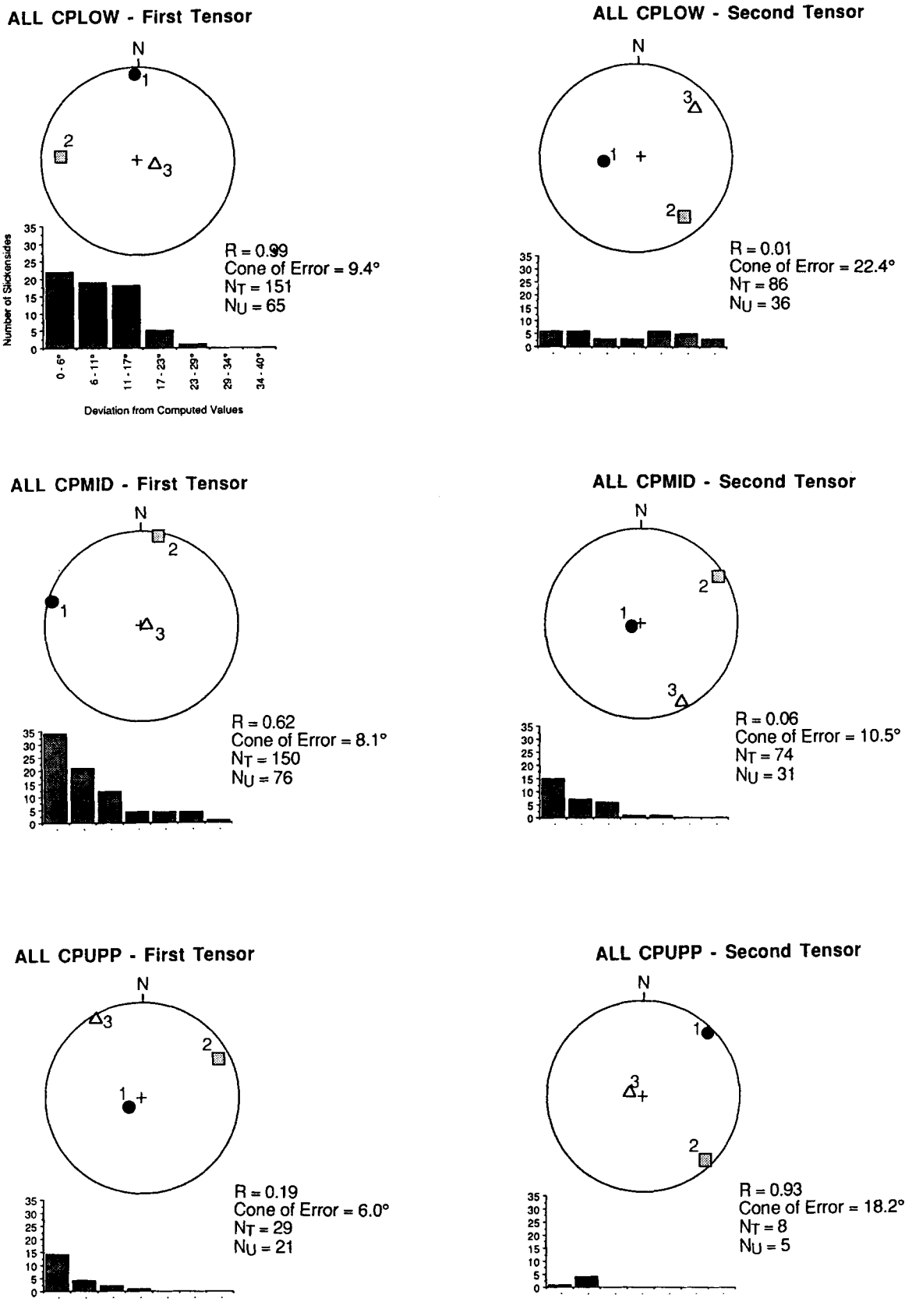

Fig. 5. Stereographic projections giving the orientations of paleostress principal directions calculated for different subdivisions of the Cumberland Plateau (CP) thrust zone. Thrust dip direction in this zone is 110/02°, azimuth of sheet transport = 280°. 1, 2 and 3 represent the three principal compressive directions, with 1 having the greatest and 3 the least magnitudes. Histograms give the angular deviations of fault–slickenside data pairs used to compute each tensor. Axes for all histograms are as labeled in 'ALL CPLOW—First Tensor' diagram. $R = (\sigma_2 - \sigma_3)/(\sigma_1 - \sigma_3)$. NU is the number of fault–slickenside pairs actually used to compute a given paleostress tensor. NT is the total number of fault–slickenside pairs that could constrain tensors during each program iteration. After one program iteration, NT is equal to the grand total of data pairs minus those used to compute tensors in earlier iterations. The relative ages of the tensors, i.e. 'first' or 'second' depends on cross-cutting patterns of faults, not the order in which the program extracted them.

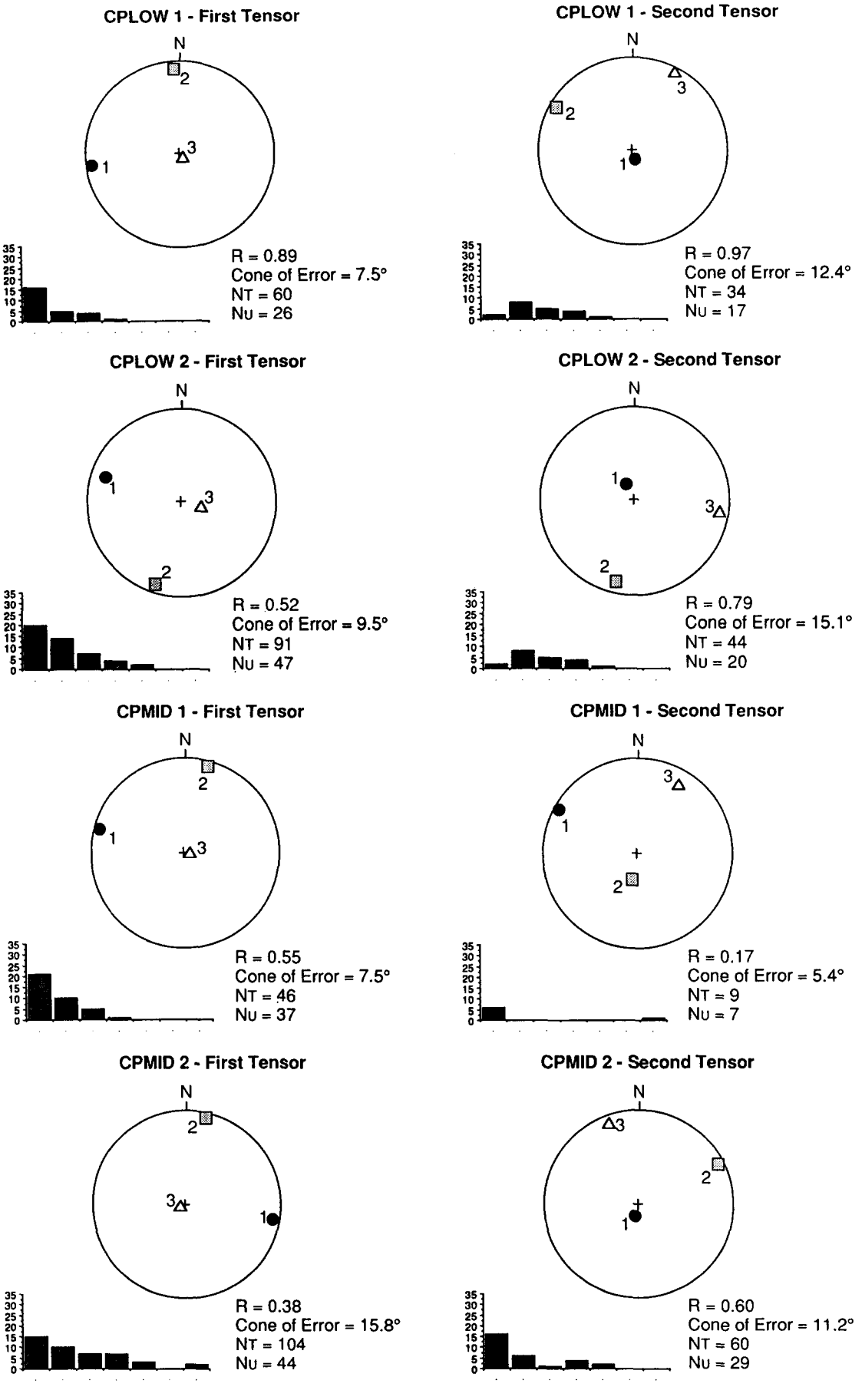
CPLOW 1 - First Tensor
R = 0.89
Cone of Error = 7.5°
NT = 60
Nu = 26
CPLOW 1 - Second Tensor
R = 0.97
Cone of Error = 12.4°
NT = 34
Nu = 17
CPLOW 2 - First Tensor
R = 0.52
Cone of Error = 9.5°
NT = 91
Nu = 47
CPLOW 2 - Second Tensor
R = 0.79
Cone of Error = 15.1°
NT = 44
Nu = 20
CPMID 1 - First Tensor
R = 0.55
Cone of Error = 7.5°
NT = 46
Nu = 37
CPMID 1 - Second Tensor
R = 0.17
Cone of Error = 5.4°
NT = 9
Nu = 7
CPMID 2 - First Tensor
R = 0.38
Cone of Error = 15.8°
NT = 104
Nu = 44
CPMID 2 - Second Tensor
R = 0.60
Cone of Error = 11.2°
NT = 60
Nu = 29

Fig. 5 (*contd*).

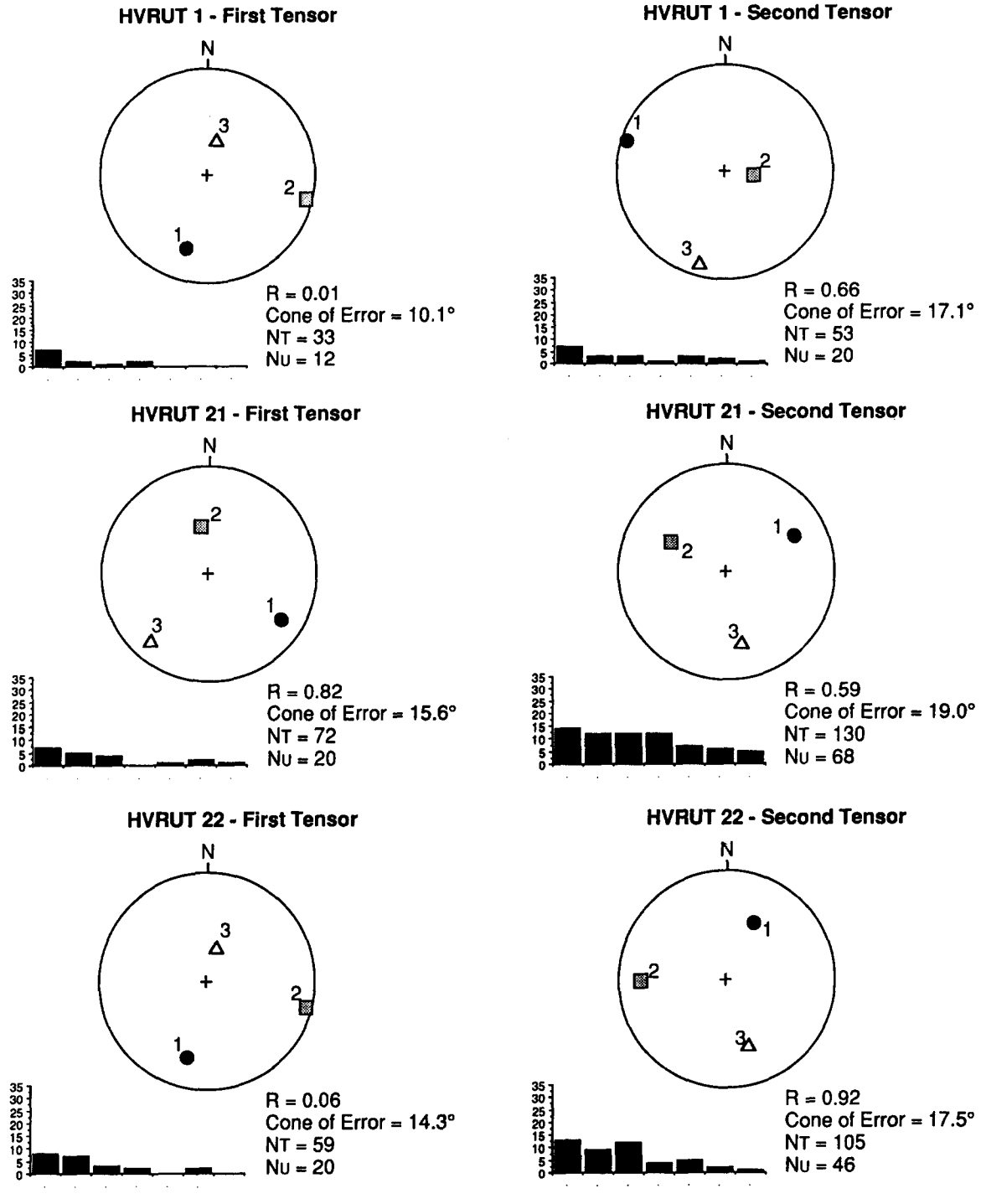

Fig. 6. Stereographic projections giving the orientations of paleostress principal directions calculated for the Hunter Valley (HV) thrust zone. Thrust dip direction in this zone is 140/25°, azimuth of sheet transport = 338°. See Fig. 5 for complete legend.

with fault reorientation responsible for some multiple or overprinted slip lineations. Faults no longer favorably oriented for slip, either because they rotated relative to the principal stress directions or because the principal stresses changed, apparently became inactive without losing information on earlier slip episodes. Thus, low-angle faults were active as long as their resolved shear stresses remained sufficiently high. When the principal stresses changed sufficiently, high-angle faults formed and accrued slip. Slip on high-angle faults apparently did not obscure geometric patterns associated with earlier increments.

Fault–slickenside measurements not compatible with paleostress tensors are typically those from small faults confined to individual blocks (Fig. 7). Small fault–slickenside pairs may have once been compatible with the principal stress directions indicated by block-bounding faults and rotated relative to them during finite slip on the bounding faults. Unfortunately, we have no good evidence to indicate which paleostress

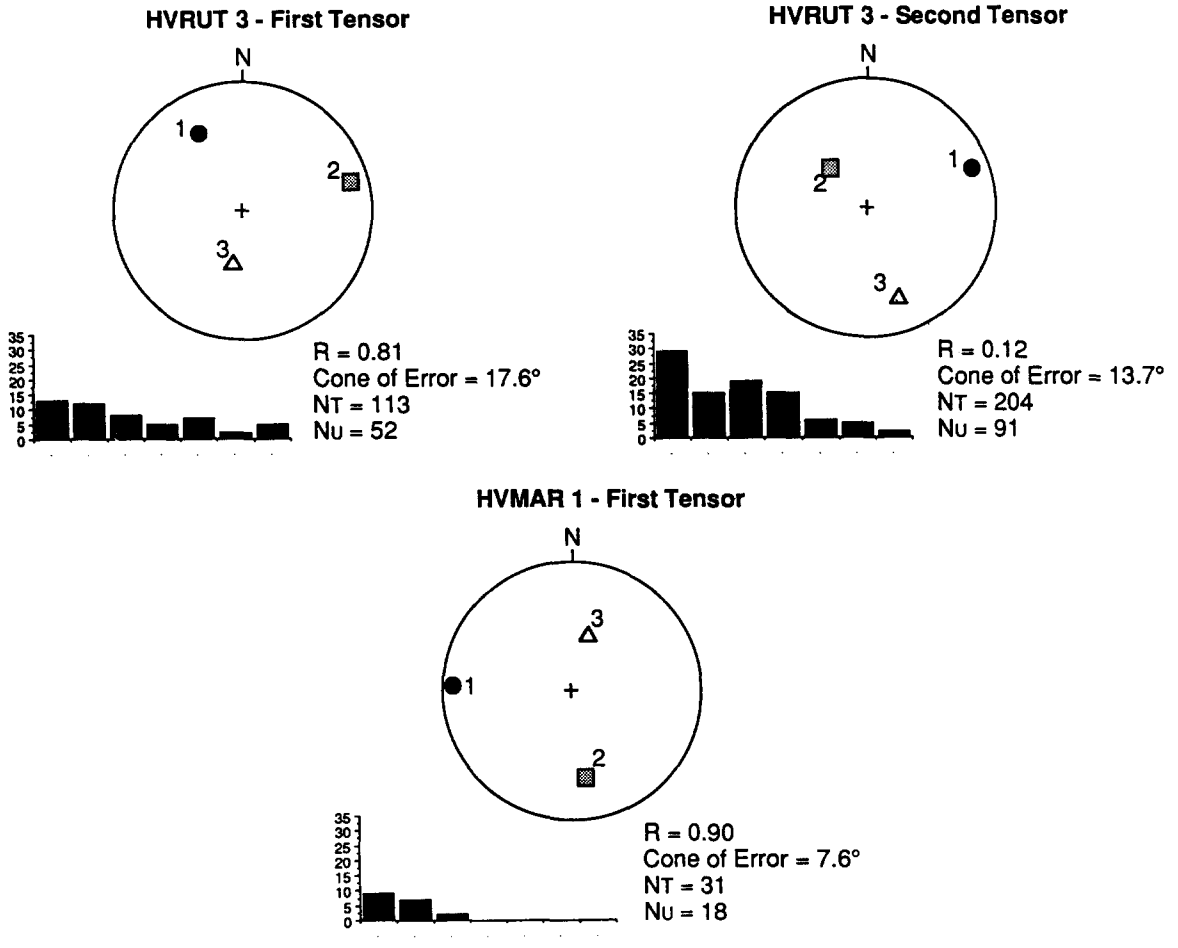

Fig. 6 (*contd*).

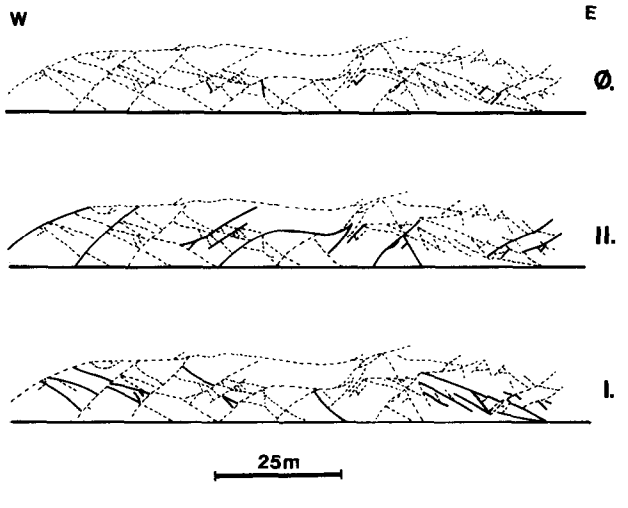

Fig. 7. Tracings of the down-plunge projection of the CP thrust zone, showing a part of the CPLOW1 subdivision; each section shows all faults whose outcrop length exceeds 1 m. In the bottom (I.), solid lines are faults that constrain the first CPLOW tensor. In the middle tracing (II.), solid lines are faults that constrain the second CPLOW tensor. In the upper tracing (Ø.), solid lines are faults that do not conform with either CPLOW paleostress tensor. Those faults dashed in all three tracings are those for which we measured no slickensides. Note the paucity of 'large' minor faults (those with outcrop lengths greater than 1 m) that do not conform with either tensor. Similar effects occur in all subdivisions of both thrust zones.

tensor is more nearly compatible with each small fault, thereby allowing us to calculate the fault's rotation. Alternatively, small faults may have formed in response to local stress variations near steps in, or the growing tips of, block-bounding faults (cf. Segall & Pollard 1980). If transient local stress inhomogeneities existed, the stress histories of these faulted rocks were more complex than envisioned by Wallace (1951), Bott (1959) or Carey & Brunier (1974). We cannot distinguish which of these possible effects, if either, is more significant in our data.

In the CP thrust zone, the maximum and minimum paleostress and finite strain principal axes lie in the same *a–c* plane: perpendicular to the thrust and parallel to transport. Paleostress and strain principal directions have different pitches within that plane, indicating that strain was non-coaxial. In the 10 m thick region immediately above the thrust (CPLOW), paleostress and finite strain principal directions are not parallel in part because finite strains resulted from (1) shortening offsets on low-angle faults, then (2) elongational offsets on high-angle faults. The principal directions of strain due only to offsets on low-angle faults, estimated by restoring offsets on high-angle faults, are also oblique to the principal directions of paleostress tensors constrained by low-angle faults, indicating that the shortening strains alone were non-coaxial. A similar obliquity between paleostress and strain principal directions pertains to

deformation accommodated by low-angle faults in the middle region and that accommodated by high-angle faults in the lower region (Fig. 7). In all cases, strains are non-coaxial largely because fault slip was partitioned mainly onto one of the several fault sets compatible with the paleostress tensors. Factors other than stress magnitudes or orientations, either the thrust-zone-wide displacement gradient associated with sheet movement, or fault interactions as finite strains accrued (cf. Jackson 1987), affected which faults remained active here. The correlation of widely different shear strain magnitudes (at different positions within this thrust zone) with paleostress tensors having similar principal directions may be due to one of several causes. First, our initial paleostress tensor may not record the earliest stress in the thrust zone. Second, spatial variations in displacements due to movement of the thrust sheet, not spatial variations in the stresses, may have produced the observed strain gradients. In this case, deformation might have accrued in a setting comparable to that in a perfectly plastic body where differential stresses are everywhere equal to the material's yield strength but local strain rates, and therefore local strain magnitudes, vary with position in the body. Third, there may have been steep gradients in absolute stress magnitudes that produced the observed strain gradients. Fourth, steep gradients in rock strength within the thrust zone may have produced the observed strain gradients.

These four factors may contribute to disparities between the relative magnitudes of the paleostress and strain principal values, but other factors also pertain here. Paleostress tensors measured in two regions near the CP thrust where faults and slickensides have very similar attitudes (CPLOW1 and CPLOW2) have σ_1 subhorizontal and parallel to transport, σ_2 subhorizontal and normal to transport, and σ_1 and σ_2 nearly equal in magnitude (Fig. 5). Strain data indicate that strata in both regions shortened subparallel to transport and elongated normal to transport (Wojtal 1986), with shortening in transport much greater than elongation normal to transport. Combining fault–slickenside data from the two regions yields a paleostress tensor with σ_1 normal to transport (ALL CPLOW, Fig. 5). Strain data conform with the paleostress tensors from the individual regions, not with that from the composite region, even though the data set for the composite region is larger. In the middle regions of the CP thrust zone, high-angle faults are less pervasive and deformation is more nearly plane strain. The symmetry of computed paleostress tensors did not switch when we combined data from two middle regions with similar fault patterns (CPMID1 + CPMID2 = ALL CPMID), even though many faults in these regions have large offsets and fault density is locally high. This discrepancy points out an important caveat for paleostress analyses. Computed relative magnitudes of paleostress principal values depend upon how fault–slickenside pairs are distributed about the Mohr circles. Ideally, fault–slickenside pairs define the entire circumferences of the Mohr circles, indicating that faults and slickenside with ranges of orientations constrain the computed tensor. Fault–slickenside pairs in our data cluster along limited segments of the Mohr circles (Fig. 8), a distribution that may indicate calculated R values are suspect. Moreover, this example underscores the importance of corroborative geological evidence in interpreting the computer output. In this case, azimuths of the best-fit principal values are, as far as can be tested, reliable, whereas their relative magnitudes are correct only within the range of error.

In the CP thrust zone, where 'block-boundary sliding' deformation is mesoscopically homogeneous, computed errors in the orientations of paleostress principal directions are relatively small. In the HV thrust zone, where the block-boundary sliding deformation is not mesoscopically homogeneous and intra-block deformation is more extensive, computed errors in orientations of paleostress principal diections are relatively large. Among the factors that may decrease the precision of paleostress analysis are: (1) slip on two types of high-angle fault that rotated earlier fault–slickenside pairs farther from their initial orientations; (2) sizeable intra-block deformation that accommodated large slip on block-bounding faults, causing numerous small faults to rotate and deactivate; or (3) sizeable continuous strain that accompanied block-boundary sliding (cf. Cooper *et al.* 1983), causing fault–slickenside pairs to rotate from ideal orientations.

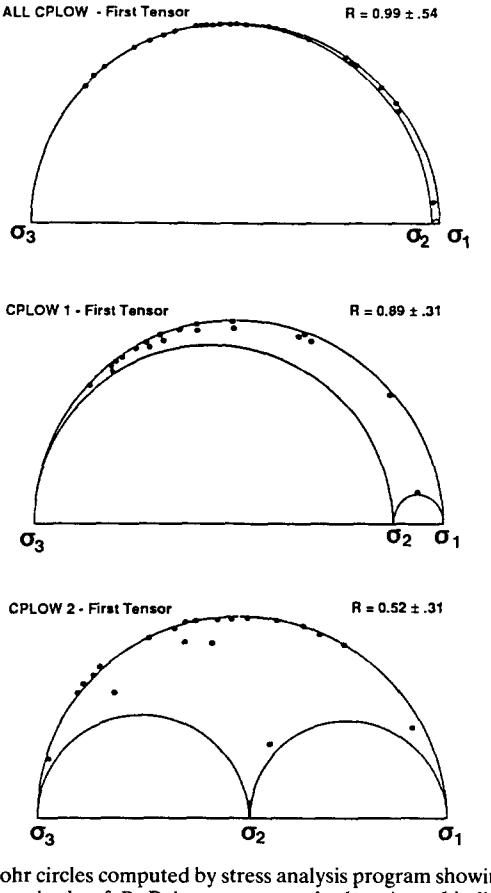

Fig. 8. Mohr circles computed by stress analysis program showing the relative magnitude of R. Points represent the location of individual fault–slickenside pairs on the Mohr diagram. Many points represent multiple data pairs. Clustering of faults along particular segments of the diagram limit the accuracy of the R values, and result in the large errors computed for them.

Paleostress tensors for the HV thrust zone define an *a–c* principal plane comparable to that defined in the CP thrust zone: normal to the thrust and parallel to transport. Paleostress principal directions in this plane also indicate (1) transport-parallel and nearly thrust-parallel compression, and (2) transport-parallel and nearly thrust-parallel extension with thrust-normal compression (tensors in region HVRUT22 conform with this interpretation if the R values are not precise). Based on cross-cutting relationships between the faults that define the different tensors, thrust-parallel compression preceded thrust-parallel extension. Slightly large numbers of minor faults in the HV thrust zone do not conform with either of the two well-defined tensors, and some of the residual fault–slickenside pairs are compatible with poorly defined tensors for shortening and elongation oblique to transport. Movement on high-angle faults oblique to the thrust strike may, then, account for some of the error in the HV tensors.

If the paleostress principal directions (incremental strain directions) in these thrust zones do correspond to loading situations, both thrust zones experienced similar stress histories. A sequence of thrust-parallel compression followed by thrust-parallel extension is compatible with sheet movement past an asperity in a thrust zone (Platt & Leggett 1986, Woodward *et al.* 1988) or with the passage of a surge through the thrust sheet (Sharp *et al.* 1988). Our measured paleostress tensors indicate that (1) the resolved shear stress magnitudes on the major thrust surface were low, and (2) a simple Mohr–Coulomb analysis cannot adequately explain the orientation of the thrust fracture. These data corroborate the results of regional studies of stresses in the vicinity of active strike-slip faults (cf. Mount & Suppe 1987), and raise similar questions regarding the mechanics of slip on surfaces with sizeable normal stress and low shear stress magnitudes. Thrust slip at low shear stress magnitudes is compatible with low resistance to frictional sliding due to elevated pore-fluid pressures (Hubbert & Rubey 1959, Davis *et al.* 1983) or with the flow of weak rocks in the fault zone (Chapple 1978, Wojtal & Mitra 1986, 1988). Inferences in thrust movement mechanisms are guided by, and in turn guide, inferences on whether deformation by arrays of minor faults is best described as viscous or brittle.

CONCLUSIONS

Our analysis of arrays of minor faults with finite displacements yields paleostress tensors that appear to be well-constrained. In the CP thrust zone, we can compare the directions and magnitudes of principle paleostresses with the directions and magnitudes of principal finite strains. Paleostress tensors and strains share a principal plane, but paleostress principal directions in that plane are oblique to strain principal directions. This obliquity is consistent with strongly noncoaxial deformation, but difficult to reconcile with stress-based models for fault slip. The obliquity is consistent with the displacement boundary conditions in these thrust zones. Changes in R values computed for paleostress tensors correlate weakly with changes in the shape of the finite strain ellipsoid.

Inasmuch as we are able to judge by objective criteria, paleostress analysis is viable in these settings. We are satisfied that paleostress analyses identify that fraction of a collection of faults that worked together to accommodate a particular strain increment. When fault offsets are large, however, relating the principal directions of strain to paleostress vectors must be done carefully. The primary caution derives from the difficulty, particularly when fault offsets are large, in inferring unequivocally from slickenlines on a fault the resolved shear stress on that plane. We feel that paleostress principal directions are best interpreted as incremental strain directions; in Levy–Mises materials the incremental strain principal directions give paleostress principal directions. The success of paleostress analyses at inferring incremental strain directions, even when fault slips are large and many of its preconditions are violated, suggests that the technique may be less significantly affected by minor deviations from the ideal case envisioned by Carey & Brunier (1974).

If our paleostress tensors correspond to tectonic loads, (1) both thrust zones experienced earlier transport- and thrust-parallel compression and later transport- and thrust-parallel extension, and (2) resolved shear stresses on major thrust surfaces were relatively small during both deformation increments.

Acknowledgements—We thank our colleagues at the University of Minnesota, particularly Christian Teyssier and Peter Hudleston, for thoughtful discussions of paleostress analysis. We also thank Z. Reches and A. Etchecopar for careful reviews that enabled us to improve substantially this contribution. Sue Treagus's scientific and editorial suggestions helped us to clarify our presentation.

REFERENCES

Anderson, E. M. 1951. *The Dynamics of Faulting*. Oliver and Boyd, Edinburgh.

Angelier, J. 1979. Determination of the mean principal directions of stresses for a given fault population. *Tectonophysics* **56**, T17-T26.

Angelier, J. 1984. Tectonic analysis of fault slip data sets. *J. geophys. Res.* **89**, 5835–5848.

Angelier, J. & Mechler, P. 1977. Sur un méthode graphique de récherche des constraintes principales également utilisable et en seismologie. *Bull. Soc. géol. Fr.* **19**, 1306–1318.

Angelier, J., Tarantola, A., Valette, B. & Manoussis, S. 1982. Inversion of field data in fault tectonics to obtain the regional stress. I—Single phase fault populations: a new method of computing the stress tensor. *Geophys. J. R. astr. Soc.* **69**, 607–621.

Armijo, R. & Cisternas, A. 1978. Un problème inverse en microtechnique cassante. *C. r. Acad. Sci., Paris* **287**, 595–598.

Arthaud, F. 1969. Méthode de détermination graphique des directions de raccourcissement, d'allongement et intermédiaire d'une population de failles. *Bull. Soc. géol. Fr.* **XI**, 729–732.

Arthaud, R. & Mattauer, M. 1969. Exemples de stylolites d'origine tectonique dans le Languedoc, leurs rélations avec la tectonique cassante. *Bull. Soc. géol. Fr.* **XI**, 738–744.

Aydin, A. & Reches, Z. 1982. Number and orientation of fault sets in the field and in experiments. *Geology* **10**, 107–112.

Bott, M. H. P. 1959. The mechanics of oblique slip faulting. *Geol. Mag.* **96**, 109–117.

Carey, E. 1979. Récherche des directions principales de contraintes associées au jeu d'une population de failles. *Rev. Geogr. phys. Geol. dyn.* **21**, 57–66.

Carey, E. & Brunier, B. 1974. Analyse théoretique et numérique d'un modèle mécanique élémentaire appliqué a l'étude d'une population de failles. *C. r. Acad. Sci., Paris* **279**, 891–894.

Chapple, W. M. 1978. Mechanics of thin-skinned fold and thrust belts. *Bull. geol. Soc. Am.* **89**, 1189–1198.

Cooper, M. A., Gorton, M. R. & Hossack, J. R. 1983. The origin of the Basse Normandie duplex, Bovlonnais, France. *J. Struct. Geol.* **5**, 139–153.

Davis, D., Suppe, J. & Dahlen, F. A. 1983. Mechanics of fold-and-thrust belts and accretionary wedges. *J. geophys. Res.* **88**, 1153–1172.

Elliott, D. 1976. The energy balance and deformation mechanisms of thrust sheets. *Phil. Trans. R. Soc. Lond.* **A283**, 289–312.

Ellsworth, W. L. 1982. A general theory for determining the state of stress in the earth from fault slip measurements. *Terra Cognita* **2**, 170–171.

Etchecopar, A. Vasseur, G. & Daignieres, M. 1981. An inverse problem in microtectonics for the determinination of stress tensors from fault striation analysis. *J. Struct. Geol.* **3**, 51–65.

Ford, H. 1963. *Advanced Mechanics of Materials*. Longmans, Green and Co., London.

Gamond, J. F. 1987. Bridge structures as sense of displacement criteria in brittle fault zones. *J. Struct. Geol.* **9**, 609–620.

Gay, N. C. 1970. The formation of step structures on slickensided fault surfaces. *J. Geol.* **78**, 523–532.

Gretener, P. E., 1972. Thoughts on overthrust faulting in a layered sequence. *Bull. Can. Petrol. Geol.* **20**, 583–607.

Handin, J. 1969. On the Coulomb–Mohr failure criterion. *J. geophys. Res.* **74**, 5343–5348.

Harris, L. D. & Milici, R. C. 1977. Characteristics of thin-skinned style of deformation in the southern Appalachians and potential hydrocarbon traps. *Prof. Pap. U.S. geol. Surv.* **1018**, 1–40.

Hubbert, M. K. & Rubey, W. W. 1959. Role of fluid pressure in mechanics of overthrust faulting. *Bull. geol. Soc. Am.* **70**, 115–166.

Jackson, J. A. 1987. Active normal faulting and crustal extension. In: *Continental Extension Tectonics* (edited by Coward, M. P., Dewey, J. F. & Hancock, P. L.). *Spec. Publs geol. Soc. Lond.* **28**, 3–17.

Kleinspehn, K., Pershing, J. & Teyssier, C. 1989. Paleostress stratigraphy: a new technique for analyzing tectonic control on sedimentary-basin subsidence. *Geology* **17**, 253–257.

Mandal, N. & Chakraborty, C. 1989. Fault motion and curved slickenlines: a theoretical analysis. *J. Struct. Geol.* **11**, 497–502.

Means, W. D. 1987. A newly recognized type of slickenside striation. *J. Struct. Geol.* **9**, 585–590.

Michael, A. J. 1984. Determination of stress from slip data: faults and folds. *J. geophys. Res.* **89**, 11,517–11,526.

Milici, R. C. 1963. Low-angle overthrust faulting, as illustrated by the Cumberland Plateau–Sequatchie Valley fault system. *Am. J. Sci.* **261**, 815–825.

Mount, V. S. & Suppe, J. 1987. State of stress near the San Andreas Fault: Implications for wrench tectonics. *Geology* **15**, 1143–1146.

Norris, D. K. & Barron, K. 1968. Structural analysis of features on natural and artificial faults. In: *Research in Tectonics* (edited by Baer, A. J. & Norris, D. K.). *Geol. Surv. Pap. Can.* **68-52**, 136–172.

Petit, J. P. 1987. Criteria for the sense of movement on fault surfaces in brittle rocks. *J. Struct. Geol.* **9**, 597–608.

Platt, J. P. & Leggett, J. K. 1986. Stratal extension in thrust footwalls; Makran accretionary prism: implications for thrust tectonics. *Bull. Am. Ass. Petrol. Geol.* **70**, 191–203.

Ramsay, J. G. & Huber, M. I. 1983. *The Techniques of Modern Structural Geology, Volume 1: Strain Analysis*. Academic Press, London.

Reches, Z. 1978. Analysis of faulting in a three-dimensional strain field. *Tectonophysics* **47**, 109–129.

Reches, Z. 1983. Faulting of rocks in three-dimensional strain fields. II. Theorectical analysis. *Tectonophysics* **95**, 133–156.

Reches, Z. 1987. Determination of the tectonic stress tensor from slip along faults that obey the Coulomb yield condition. *Tectonics* **6**, 849–861.

Reches, Z. & Dieterich, J. H. 1983. Faulting of rocks in three-dimensional strain fields. I. Failure of rocks in polyaxial, servo-controlled experiments. *Tectonophysics* **95**, 111–132.

Rich, J. L. 1934. Mechanics of low-angle overthrust faulting as illustrated by Cumberland thrust block, Virginia, Kentucky and Tennessee. *Bull. Am. Ass. Petrol. Geol.* **18**, 1584–1596.

Rodgers, J. 1970. *The Tectonics of the Appalachians*. Interscience, New York.

Rutter, E. H. & Mainprice, D. H. 1978. The effect of water on stress relaxation of faulted and unfaulted sandstone. *Pure & Appl. Geophys.* **116**, 634–654.

Segall, P. & Pollard, D. D. 1980. Mechanics of discontinuous faults. *J. geophys. Res.* **85**, 4337–4350.

Sharp, M., Lawson, W. & Anderson, R. S. 1988. Tectonic processes in surge-type glacier. *J. Struct. Geol.* **10**, 499–516.

Shimamoto, T. 1986. Transition between frictional slip and ductile flow for halite shear zones at room temperature. *Science* **231**, 711–715.

Stearns, R. G. 1954. The Cumberland Plateau overthrust and the geology of the Crab Orchard Mountains. *Bull. Tenn. Div. Geol.* **60**, 1–47.

Tjia, H. D. 1964. Slickensides and fault movement. *Bull. geol. Soc. Am.* **75**, 683–686.

Tjia, H. D. 1967. Sense of fault displacements. *Geologie Mijnb.* **46**, 392–396.

Wallace, R. E. 1951. Geometry of shearing stress and relation to faulting. *J. Geol.* **59**, 118–130.

Wojtal, S. F. 1982. Finite deformation in thrust sheets and their material properties. Unpublished Ph.D. dissertation, Johns Hopkins University, Baltimore, Maryland.

Wojtal, S. 1986. Deformation within foreland thrust sheets by populations of minor faults. *J. Struct. Geol.* **8**, 341–360.

Wojtal, S. 1989a. Measuring displacement gradients and strain in faulted rocks. *J. Struct. Geol.* **11**, 669–678.

Wojtal, S. 1989b. Day Seven—Valley and Ridge Province in southwest Virginia and northeast Tennessee. In: *Geometries and Deformation Fabrics in the Central and Southern Appalachian Valley and Ridge and Blue Ridge* (edited by Woodward, N. B.). *Guidebook for Int. Geol. Cong. Field Trip* **357**, 57–68.

Wojtal, S. & Mitra, G. 1986. Strain hardening and strain softening in fault zones from foreland thrusts. *Bull. geol. Soc. Am.* **97**, 674–687.

Wojtal, S. & Mitra, G. 1988. Nature of deformation in some fault rocks from Appalachian thrusts. In: *Geometries and Mechanisms of Thrusting with Special Reference to the Appalachians* (edited by Mitra, G. & Wojtal, S.). *Spec. Pap. geol. Soc. Am.* **222**, 17–33.

Woodward, N. B., Wojtal, S., Paul, J. B. & Zadins, Z. 1988. Partitioning of deformation within several external thrust zones of the Appalachian orogen. *J. Geol.* **96**, 351–361.